



# Spatial and temporal patterns of propagation from meteorological to hydrological droughts in Brazil

Alena G. Bevacqua<sup>a</sup>, Pedro L.B. Chaffe<sup>b,c,\*</sup>, Vinicius B.P. Chagas<sup>a</sup>, Amir AghaKouchak<sup>c,d</sup>

<sup>a</sup> Graduate Program of Environmental Engineering, Federal University of Santa Catarina, Florianopolis, Brazil

<sup>b</sup> Department of Sanitary and Environmental Engineering, Federal University of Santa Catarina, Florianopolis, Brazil

<sup>c</sup> Department of Civil and Environmental Engineering, University of California, Irvine, USA

<sup>d</sup> Department of Earth System Science, University of California, Irvine, USA

## ARTICLE INFO

This manuscript was handled by Andras Barossy, Editor-in-Chief

### Keywords:

Drought propagation  
Meteorological drought  
Hydrological drought  
Standardized drought indices  
Brazil

## ABSTRACT

Meteorological droughts propagate through the hydrological cycle causing hydrological droughts and societal impacts. However, the effects of climate and basin characteristics on hydrologic drought propagation vary regionally and remain largely unclear. In this paper, we characterize meteorological and hydrological droughts in 457 basins in Brazil. Using the Standardized Precipitation Evapotranspiration Index (SPEI) and Standardized Streamflow Index (SSI), we investigate hydrologic drought propagation based on differences in drought onset, the center of mass, and time to peak. Additionally, we estimate the recovery time of meteorological and hydrologic drought events. The results indicate that hydrological droughts are usually more long-lasting, severe, and with a slower recovery time compared to meteorological droughts. While the most severe meteorological droughts are observed in humid regions (e.g., Amazon and Southern Brazil), the most severe and long-lasting hydrological droughts are found in the driest region (i.e., Northeast Brazil) or mostly impacted by human activities (i.e., Southeast Brazil). Hydrological droughts in dry regions can take four times longer to recover than meteorological ones. For most regions, the propagation time was slightly different considering the different approaches. Our results highlight the importance of a multi-indicator approach to fully characterize the mechanisms controlling the development and propagation of droughts through the water cycle.

## 1. Introduction

Droughts are associated with major economic losses and damages to the ecosystem (Wilhite, 2000). Between 1970 and 2012, droughts were responsible for approximately one-third of deaths related to natural disasters and an economic loss of 200 billion dollars worldwide (WMO, 2014). They threaten food production, energy generation, water supply, and can intensify wildfires and tree mortality (Doughty et al., 2015; Melo et al., 2016; Taufik et al., 2017; Brás et al., 2019). Thus, improving drought characterization is crucial to enhance its monitoring, management, and prediction.

Drought is defined as the period in which water availability is below what would be normally expected and fails to meet human or environmental needs (Wilhite and Pulwarty, 2018). These events are broadly classified into four categories (Wilhite and Glantz, 1985): (i) meteorological drought, associated with negative anomalies in precipitation; (ii) agricultural drought, related to a decline in soil moisture; (iii)

hydrological drought, when there is a deficit in the streamflow; (iv) socio-economic drought when events have socio-economic impacts. Several drought indices have been developed to identify, characterize, and compare these events. For example, the World Meteorological Organization (WMO) recommends the Standardized Precipitation Index (SPI; McKee et al., 1993) for monitoring meteorological droughts (Hayes et al., 2011). For hydrological droughts, the Standardized Streamflow Index (SSI; Shukla and Wood, 2008; Vicente-Serrano et al., 2012) is commonly used. Yet, since droughts are related to more than a single variable, using only one variable index may lead to an incomplete analysis. Therefore, several multivariate indices have been created (Vicente-Serrano et al., 2010; Hao and AghaKouchak, 2014).

Typically, negative anomalies in precipitation propagate slowly through the hydrological cycle, giving rise to hydrological drought. This process is denoted as drought propagation (Eltahir and Yeh, 1999) and depends on the climate, biophysical and geographic properties of the region, as well as anthropogenic influences (Wu et al., 2021). It is well-

\* Corresponding author at: Department of Sanitary and Environmental Engineering, Federal University of Santa Catarina, Florianopolis, Brazil.

E-mail address: [pedro.chaffe@ufsc.br](mailto:pedro.chaffe@ufsc.br) (P.L.B. Chaffe).

known that under limited or no anthropogenic influences, drought propagation is primarily controlled by the climate and biophysical characteristics of the hydrographic basin (Van Loon, 2015; Van Lanen et al., 2013). In addition, human activities such as land cover change, dams, irrigation, and urbanization can significantly alter hydrological processes (e.g. evaporation, infiltration) and consequently drought propagation (Van Loon et al., 2016).

Numerous studies have attempted to model and understand drought propagation and its drivers (Apurv and Cai, 2020; Wu et al., 2021). Barker et al. (2016) found that in the United Kingdom, propagation time from meteorological to hydrological droughts was mostly one or two months, with basins with large aquifers showing a longer propagation time. A similar propagation time was found by Zeng et al. (2015) in the Jialing River basin. Xu et al. (2019) showed that for a basin in China, human changes such as the increase in domestic water supply and the expansion of urbanization decreased drought propagation time, while agriculture activities increased it. Land cover can also have a strong influence on the propagation time (Wu et al., 2018). Forest areas presented a longer propagation time, while pasture areas had a slower propagation for basins in China. Moreover, climate and land-use changes are the major aspects that modify drought propagation (Zhou et al., 2019). Wu et al. (2020) outlined a framework for hydrological drought recovery analysis based on a drought propagation perspective. However, the absence of a standard methodology to calculate the time of propagation and the limited understanding of how meteorological droughts develop into hydrological droughts hinders the analysis, monitoring, and development of early warning systems (Barker et al., 2016).

Brazil is particularly vulnerable to droughts given that hydroelectricity corresponds to 70% of its energy generation and irrigated agriculture is 32% of the country's water use (Getirana, 2016; Melo et al., 2016). Recently, most Brazilian regions faced the most severe and intense droughts of the last 60 years (Gunha et al., 2019). The Northeast region has suffered severe impacts due to the 2013 drought, the worst in 100 years which affected agriculture and livestock (Gutiérrez et al., 2014). In southeastern Brazil, the 2014 drought compromised the water supply of 28 million people (Melo et al., 2016). Water consumption and

climatic changes are predicted to intensify droughts even more (Marengo et al., 2017; Morales et al., 2020), threatening food security, electricity generation, and water supply (Paredes-Trejo et al., 2021; Rodrigues et al., 2020). The impacts of such changes on surface water availability and how meteorological droughts propagate to hydrological droughts in Brazil are largely unknown.

In this paper, we (i) identify and quantify meteorological and hydrological drought characteristics, (ii) estimate the recovery time for meteorological and hydrological droughts, and (iii) calculate the propagation time from meteorological to hydrological droughts in 457 hydrographic basins throughout Brazil. We use a multi-indicator approach that combines the Standardized Precipitation Evapotranspiration Index (SPEI) and the Standardized Streamflow Index (SSI) to analyze drought propagation based on differences in drought onset, the center of mass, and time to peak.

## 2. Material and methods

### 2.1. Study area

We analyze 457 hydrographic basins across the Brazilian territory (Fig. 1a). Most basin areas (51%) are between 1.500 km<sup>2</sup> and 10.000 km<sup>2</sup>, 35% of them between 10.000 km<sup>2</sup>, and 100.000 km<sup>2</sup>, and few (14%) are more than 100.000 km<sup>2</sup>. The wettest regions are the Amazon and with precipitation over 2000 mm per year (Fig. 1b) and streamflow higher than 1000 mm per year (Fig. 1c). The Northeast is the driest region, with precipitation ranging between 600 mm and 1200 mm and streamflow less than 300 mm.

### 2.2. Precipitation and streamflow data

We use daily precipitation (P) data grids from (Xavier et al., 2016) within the Brazilian territory and from Climate Prediction Center (CPC) outside the Brazilian territory. Xavier et al. (2016) dataset spatial resolution is 0.25° while the CPC dataset resolution is 0.50°. Both precipitation products were computed using interpolation of hydrometeorological gauges. Potential evapotranspiration (PET) daily

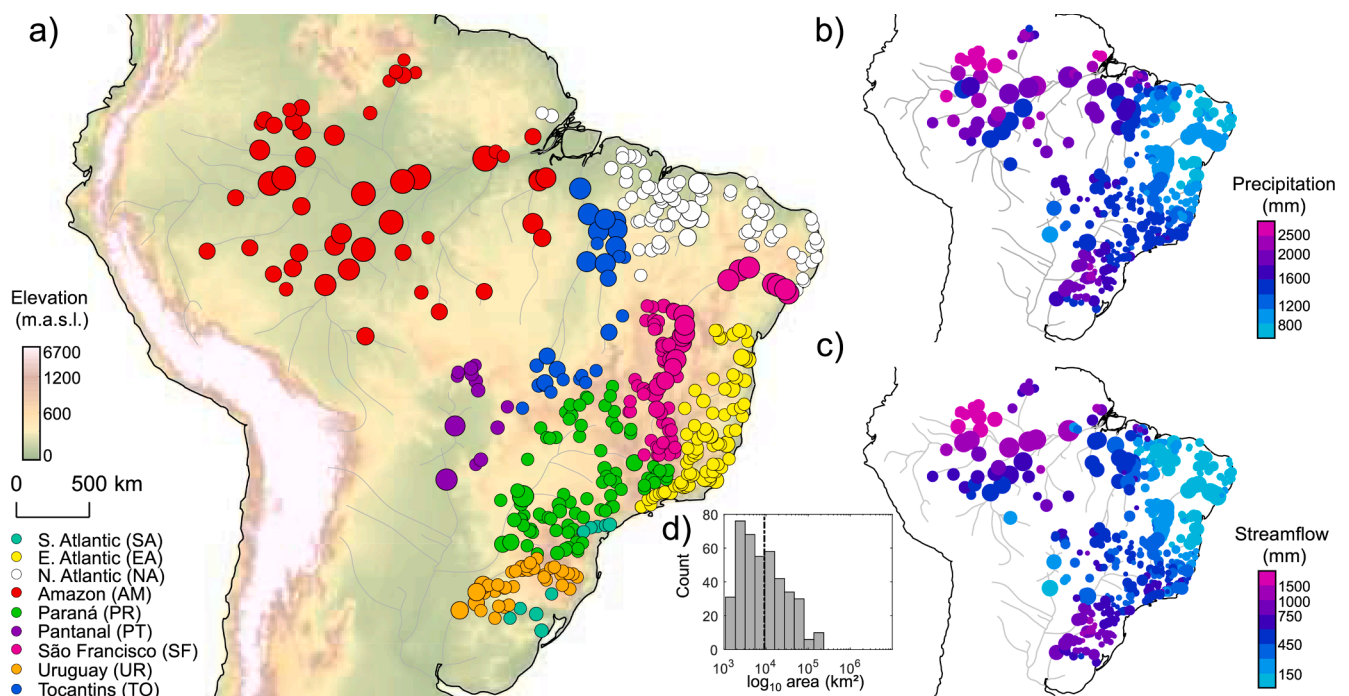


**Fig. 1.** (a) Location of the 457 streamflow gauges classified according to their hydrographic region (b) Average annual precipitation and (c) streamflow. The size of the markers is proportional to the size of the river basin. (d) Histogram of basin areas, the median (9088 km<sup>2</sup>) is represented by the dashed line.

data grid is from the Global Land Evaporation Amsterdam Model v3.3a (GLEAM; Martens et al., 2017; Miralles et al., 2011), with a resolution of 0.25°. We compute daily P and PET for each basin by averaging the cells within the basin boundaries, which we define using the digital elevation model from the SRTM (Shuttle Radar Topographic Mission; USGS, 2006). We analyze streamflow data from the CAMELS-BR dataset (Chagas et al., 2020), where only basins with less than 30% of missing data are considered and gauges with unrealistic streamflow values are removed.

### 2.3. Drought indices and characteristics

As the indicator for meteorological droughts, we use the SPEI (Vicente-Serrano et al., 2010) by estimating a simplified water balance using precipitation minus PET. We then aggregate the water balance over different timescales (1 to 12 months) and fit it to a parametric probability distribution. The drought index is obtained by using the inverse of the standard normal distribution. The SSI (Shukla and Wood, 2008; Vicente-Serrano et al., 2012) indicates hydrological droughts and its calculation follows the same principles of SPEI but only uses streamflow data. In this paper, we calculate the SPEI and SSI for the

accumulation period of 1 to 12 months. Furthermore, according to the literature recommendation, we choose the generalized extreme distribution (GEV) as the parametric distribution (Stagge et al., 2015; Vicente-Serrano et al., 2012) for both indices. SPEI- $i$  and SSI- $i$  denote the  $i$ -month (where  $i = 1, 2, \dots, 12$ ) accumulation period SPEI and SSI, respectively.

For each basin, we compute the total number of meteorological drought events, their duration, severity, and recovery time (Fig. 2a). The same computations are used for hydrological droughts using SSI. We define the start of a drought event as when the SPEI or SSI falls below the threshold of  $-1$ . The event ends when the index goes back to zero or more. Drought duration is the time from the beginning to the end of a drought event. The severity of an event is the sum of the SPEI or SSI values for each month during a drought event. The recovery time ( $r_{\text{time}}$ ) consists of how long it takes for a drought event to reach its end once it has reached its peak (Fig. 2a). The  $r_{\text{time}}$  is estimated by subtracting the peak time ( $t_{\text{peak}}$ ) by the end time ( $t_{\text{end}}$ ). We divide the recovery time of the hydrological drought by that of the meteorological drought to estimate the recovery rate for each basin, i.e., how many times more a hydrological drought takes to recover in comparison to a meteorological drought. Moreover, we use the Mann-Kendall test with a significance

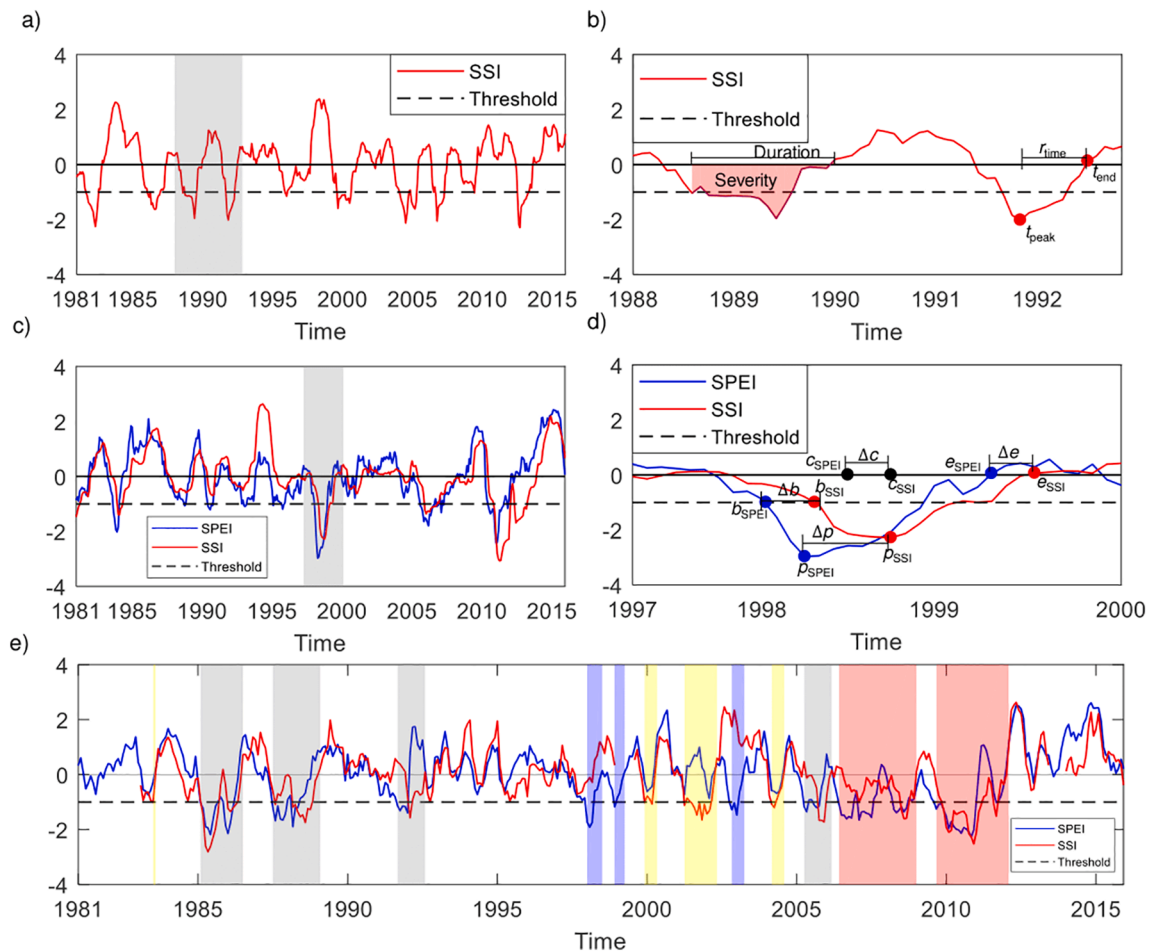


**Fig. 2.** Drought indices characteristics. (a) SSI series for 12 months timescale. The shaded grey area in (a) is detailed in (b). The characteristics of the events such as duration, severity (red shade), peak time ( $t_{\text{peak}}$ ), end time ( $t_{\text{end}}$ ), and recovery time ( $r_{\text{time}}$ ) are shown in (b). (c) An example of SPEI and SSI series. (d) The gray shaded area in (c) and the schematic of how to estimate propagation time using different indices. (e) SPEI and SSI time series showing different types of drought: hydrological drought related to one single meteorological drought (gray shaded areas), hydrological drought related to multiple meteorological droughts (red shaded areas), hydrological drought without a meteorological drought (yellow shaded areas), and meteorological droughts without a hydrological drought (blue shaded areas).  $b_{\text{SPEI}}$  and  $b_{\text{SSI}}$  are the onset time,  $p_{\text{SPEI}}$  and  $p_{\text{SSI}}$  are the peak time, and  $e_{\text{SPEI}}$  and  $e_{\text{SSI}}$  are the ending time of the meteorological (SPEI) and hydrological (SSI) drought events.  $\Delta b$ ,  $\Delta p$ , and  $\Delta e$  are the time difference between the onsets, peaks, and endings of the meteorological and hydrological droughts, respectively.  $c_{\text{SPEI}}$  and  $c_{\text{SSI}}$  are the timing of the center of mass of the meteorological and hydrological drought events and  $\Delta c$  is the difference between them. (For interpretation of the references to colour in this figure legend, the reader is referred to the web version of this article.)

level of 0.05 (Mann, 1945; Kendall, 1975) to test for trends and the Theil-Sen slope (Theil, 1950; Sen, 1968) to calculate the magnitude of trends in the SPEI and SSI series of each basin.

#### 2.4. Drought propagation

Following on from Fig. 2, we analyze the propagation from meteorological to hydrological droughts using three different methods. Following (Barker et al., 2016), we compare the SPEI and SSI series to estimate the time it takes for a precipitation deficit to affect the streamflow. This is achieved by evaluating the Pearson's correlation coefficients between the SPEI-1 to SPEI-12 series with respect to the SSI-1. To avoid potentially spurious correlations (Chatfield, 2016), the underlying trendlines in SPEI and SSI series are removed using the Theil-Sen slope (Theil, 1950; Sen, 1968).

The second method consists of calculating three indicators of the propagation time (Fig. 2b) according to: (i) the time difference between the beginnings ( $\Delta b$ ) of a meteorological and a hydrological drought event; (ii) the time difference between the peaks ( $\Delta p$ ) of those events; (iii) the time difference between the ends ( $\Delta e$ ) of those events. We analyze (i) the events in which the meteorological drought begins before the hydrological drought (ii) we considered that a hydrological drought is due to a meteorological drought if it starts before the meteorological drought ended (iii) we also analyzed just the events where the peak and the end of meteorological drought occur before the peak and end of hydrological drought (Fig. 2e).

Lastly, in the third method, we estimate the propagation time using the center of mass of the drought event. We calculate the center of mass of the same meteorological and hydrological drought events. Then, we

compute the time difference between the center of mass of the hydrological and meteorological droughts events ( $\Delta c$ ; Fig. 2b). The propagation time for each basin is the average of the time differences between the center of masses.

### 3. Results and discussion

#### 3.1. Drought characteristics

Fig. 3 shows SPEI and SSI time series at the 6-month time scale for every basin. By visually exploring the time series it becomes clear that meteorological droughts do not always lead to hydrological droughts, especially when the meteorological drought lasts for up to three months. Many short-scale meteorological droughts are attenuated by the catchment and, consequently, there are more meteorological droughts than hydrological ones. On the other hand, hydrological droughts can last longer in comparison to meteorological ones. Similar results can be seen at the time scales of 3-month and 12-month (Figs. S1 and S2).

From 2012 onwards, major long-lasting drought events have affected the southeast and the northeast regions (Gutiérrez et al., 2014; Melo et al., 2016; Marengo et al., 2017; de Brito et al., 2021). In fact, the number of drought events and their severity has become more severe in those regions, particularly in the São Francisco basin, as can be seen by the trend analysis (Fig. S3). SPEI and SSI values have been increasing in northern Amazon and southern Brazil, while they have been decreasing elsewhere. 72% of the SPEI and 76% of the SSI trends are statistically significant (significance level  $\alpha = 0.05$ ). These results are similar to Brasil Neto et al. (2021) for the SPI in the state of Paraíba in northeastern Brazil. Trends in hydrological droughts are more pronounced than those

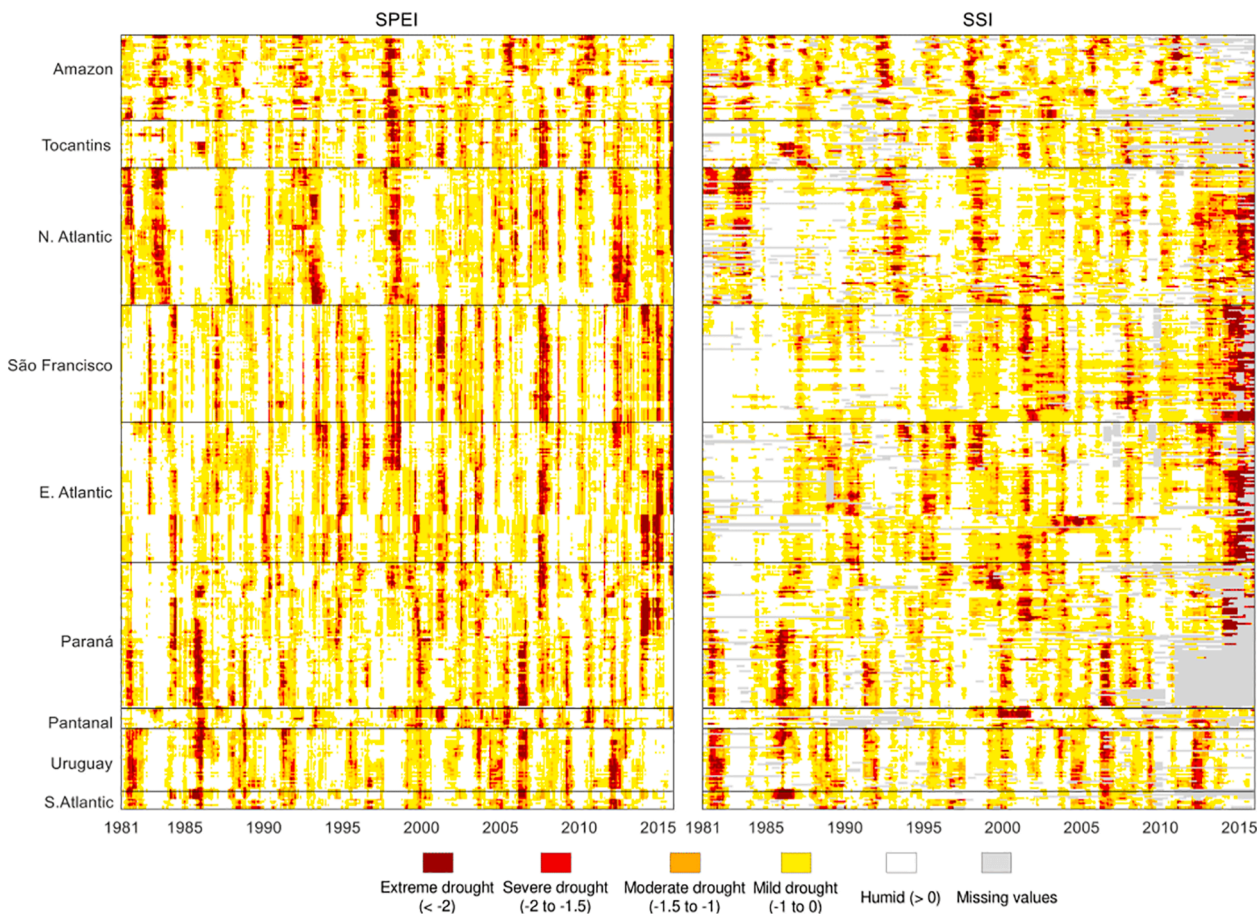


Fig. 3. Time series of drought intensity based on SPEI-6 and SSI-6 for the 457 basins analyzed. The basins are ordered according to their hydrographic region, as shown in Fig. 1.

in meteorological droughts, which implies that other drivers (e.g., land-use change and water use) also influence the development of hydrological droughts.

Meteorological droughts in Brazil are twice as frequent as hydrological droughts (Fig. 4). On average, there are 17 meteorological droughts and 8.5 hydrological droughts per basin between 1980 and 2015. On the other hand, hydrological droughts are longer (on average 14.6 months each) than meteorological droughts (on average 8.4 months each), as many sequential short-scale droughts are either pooled into a single longer hydrological drought or attenuated by the basin. As the SPEI and SSI accumulation periods increase, so do drought duration and severity, while the opposite occurs for the number of events (Fig. S5 and S6). The wet regions (Amazon and Southern Brazil) present the longest (between 10 and 15 months) and most severe meteorological droughts. The dry regions (São Francisco and Northeastern Brazil) are characterized by a high number of short meteorological droughts (between 15 and 25 events lasting from 5 to 10 months each), which are commonly grouped close to each other.

While there is a close match between spatial patterns of annual rainfall and streamflow in Brazil (i.e., Fig. 1b and c), the characteristics of hydrological droughts are substantially different than those of meteorological droughts. In fact, hydrological drought characteristics are not well explained by meteorological droughts, as the Spearman correlation between the number of meteorological and hydrological drought events is  $-0.14$  (or  $-0.15$  for the duration of events, Fig. S4). The spatial distribution of hydrological droughts is not as smooth as the meteorological ones, which indicates the fundamental importance of catchment attributes in drought propagation. Hydrological drought

severity is highly influenced by terrestrial hydrological processes and anthropogenic activities (Van Loon and Laaha, 2014). In Brazil, it has been shown that changes in land cover, such as deforestation, can intensify drought severity (Bagley et al., 2014) and that reservoirs influences drought propagation (Melo et al., 2016). Future studies should investigate those drivers of hydrological droughts.

As opposed to meteorological droughts, the longest and most severe hydrological droughts are in the Southeastern and Northeastern regions, with great variability between basins (Fig. 4). The highest differences between SPEI and SSI total number of events, average duration, and average severity occur in the São Francisco and Eastern Atlantic regions (Fig. 5). The Uruguay and the Amazon basins, on the other hand, have similar SPEI and SSI characteristics.

### 3.2. Recovery time

Fig. 6a shows that, as expected, hydrological droughts take more time to recover than meteorological droughts in most basins (77%). However, in 23% of the basins (most of them in the Amazon), the average recovery time of meteorological droughts is higher than hydrological ones. As it was observed for the drought characteristics, the average recovery times of hydrological droughts are not correlated with those from meteorological droughts (Spearman correlation of  $-0.06$ , Fig. S4). It shows that catchment attributes are also fundamental to the recovery of drought events. The recovery rate in Fig. 6b, defined here as the ratio between the average recovery time for SSI and SPEI, indicates on average how many times longer it takes for a hydrological drought to recover compared to its generating meteorological drought event. They

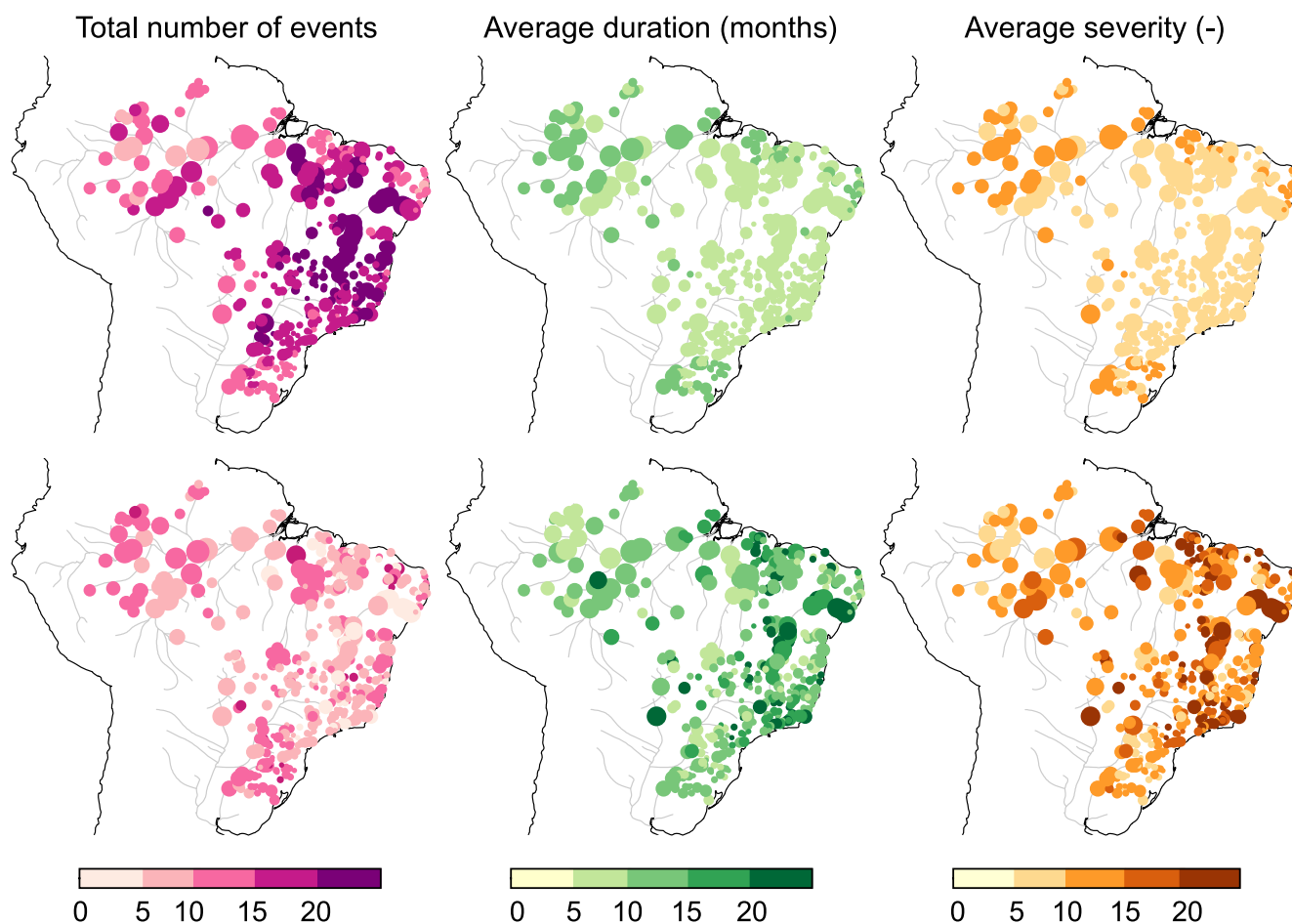


Fig. 4. Distribution of average meteorological (above) and hydrological (below) drought characteristics based on a 6-month accumulation period. The size of the markers is proportional to the size of the river basin.

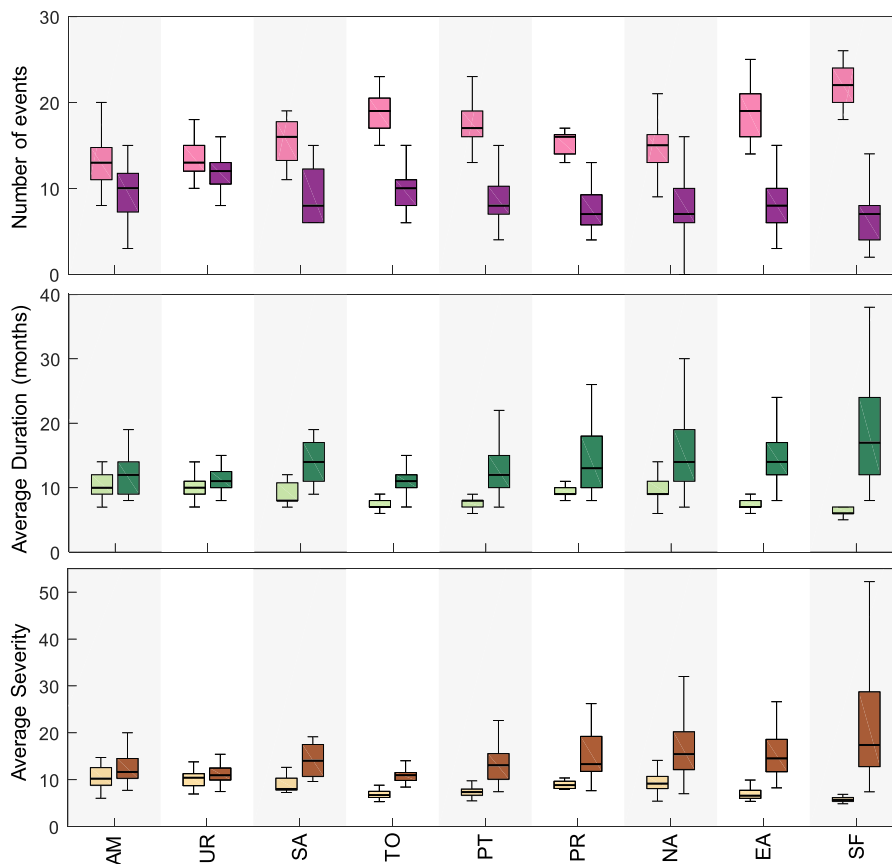


Fig. 5. Characteristics of drought events for selected regions in Brazil using SPEI and SSI with an accumulation period of 6 months. Lighter colors indicate meteorological droughts and darker colors hydrological ones.

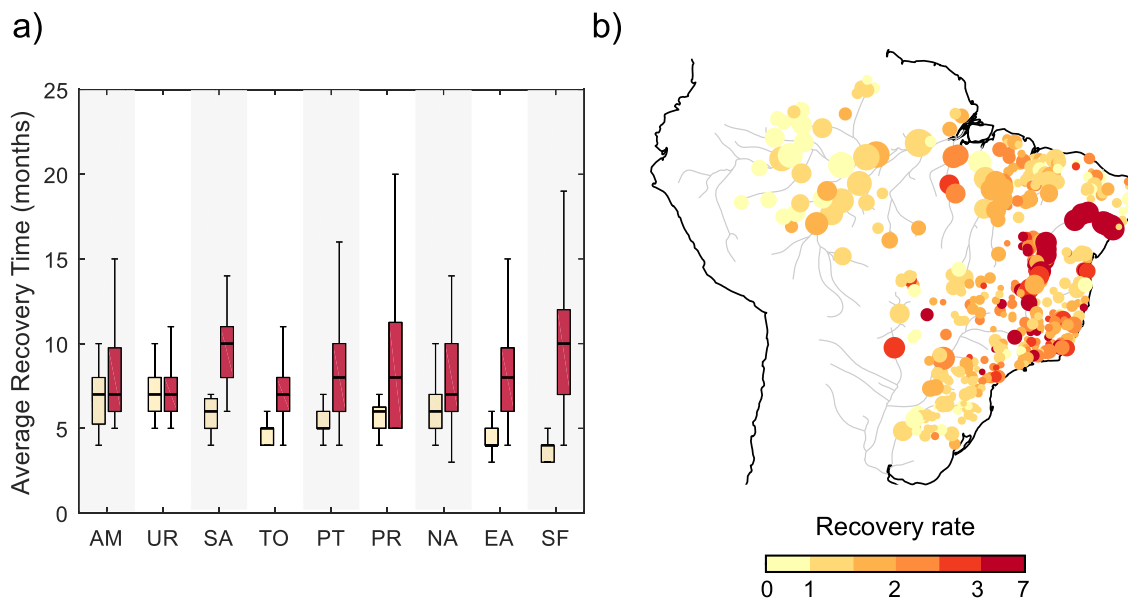


Fig. 6. Average recovery time and recovery rate of meteorological and hydrological droughts. (a) Average recovery time for SPEI-6 (lighter colors) and SSI-6 (darker colors). (b) Recovery rate, average recovery time of SSI-6 by average recovery time of SPEI-6. The size of the markers is proportional to the size of the river basin.

are between 1 and 2 for 47% of the basins, and higher than 2 for 29% of the basins. For some basins in the São Francisco region, hydrological droughts can take over four times more to recover. Again, recovery time has high spatial variability in the São Francisco, while a lower variability in the Uruguay region. We hypothesize that regions with higher

variability in recovery time are more vulnerable to droughts than the ones with lower variability.

### 3.3. Propagation time

The propagation time indices are useful indicators of the relative differences across regions; however, the absolute value of the propagation time depends completely on the method being used (Fig. 7). The propagation time using SPEI-n (Fig. 7d) considers the month accumulation with the highest correlation with SSI-1 (correlations for SPEI accumulation periods of 1 to 12 months with SSI-1 are shown in Fig. S7). The SPEI-n average value is usually between  $\Delta e$  (the longest time, as SSI takes longer to recover; Fig. 7c) and that of  $\Delta c$  and  $\Delta p$ , both of which produce similar values (Fig. 7e and b). The time to onset ( $\Delta b$ , Fig. 7a) is not a sensitive index compared to the others and provides the lowest and most smoothed out values for the propagation time. These results indicate that using the propagation time as calculated by the difference in time to onset ( $\Delta b$ ) may not be a good predictor of the time to reach the peak nor the end of a hydrological drought event in comparison to the meteorological one. Those relative differences among indices are consistent for other accumulation periods (results not shown); however, as the accumulation period increases, the average propagation time usually increases as well due to averaging effects.

The results using SPEI-n (Fig. 7d) show that while the propagation time of 2 months was the most common (119 basins), for most of the basins the propagation time was considerably higher, ranging from 6 to 12 months. These results contrast with that of Barker et al. (2016) and Zeng et al. (2015), who found a SPEI-n of 1 month for most basins in the UK and China, respectively. For the E. Atlantic, São Francisco, and the North region of Parana, in which the propagation time is predominantly high (6–12 months), high correlations are observed from the third month onwards. SPEI-n of 1 to 6 months accumulation are highly

correlated with SSI-1 in the South Atlantic, Uruguay, and the South region of Parana, indicating that the effects on the streamflow are persistent and can be noticed from the first month of drought. Additionally, there is a low correlation for these values for all accumulation periods in northern Amazon and São Francisco, which indicate either a high influence of catchment attributes or anthropogenic interference.

The E. Atlantic and São Francisco regions are the driest regions in the country and where propagation time is slower. The propagation time is relatively faster in the wetter regions such as S. Atlantic, Uruguay, northern Amazon, and Tocantins. The relationship between the propagation time, basin area, and the average annual precipitation of the basins is presented in Fig. S8. There is no clear relationship between the propagation time and the basin area, similar to what Barker et al. (2016) found for the UK basins. Moreover, differently from Barker et al. (2016), there is no relationship between the propagation time and the average annual precipitation.

The average propagation time using the difference in the onset time of the events is less than the results found for the SPEI-n, with a propagation time of fewer than 6 months for 91% of the basins (Fig. 7a). Using the difference in time of the peak, the time of propagation of 65% of the basins is also below 6 months (similar results for the difference in center of mass; Fig. 7b and e), while in the case of difference in the end time the value for most basins varies from 6 to 12 months. These results again corroborate that the onset of droughts is usually quicker and not a good estimator of time to peak and recovery. Moreover, the similar correlation found for various SPEI-n and the differences in time of propagation methods indicates the importance of considering the complexity of the drought phenomena and the several sources of uncertainty when characterizing it.

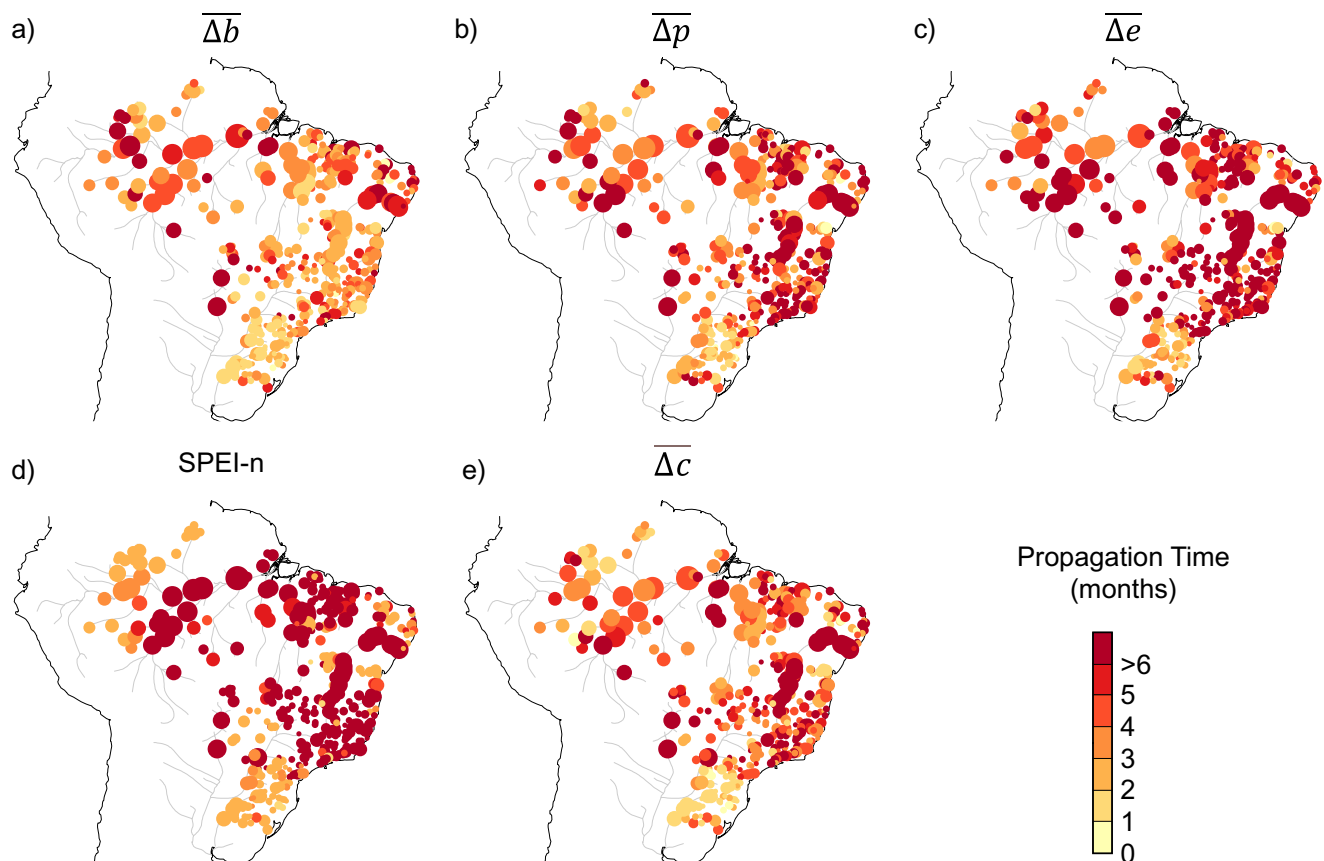


Fig. 7. Propagation time using 5 different methodologies. (a) SPEI-n with the highest correlation with SSI-1. (b) Drought propagation time calculated using the timing of the center of mass of the event. (c), (d) and (e) were calculated using the times of onset, peak, and ends of the events, respectively. The size of the markers is proportional to the size of the river basin.

#### 4. Conclusion

In this paper, we use a multi-indicator framework to identify and analyze droughts in 457 Brazilian basins. We calculate meteorological and hydrological characteristics and estimate the propagation time from meteorological to hydrological drought events by comparing different methodologies.

Our results show that meteorological droughts are more frequent and less severe than hydrological droughts in most of the territory. While short-scale meteorological drought events can be attenuated by the catchment and may ultimately not propagate to a hydrological drought, a sequence of those events may lead to longer and more severe hydrological droughts. Moreover, trends in hydrological droughts are more pronounced than what would be expected from trends in meteorological droughts alone, highlighting the importance of considering other drivers of hydrological droughts such as land and water use.

Recovery time and recovery rate vary depending on the region and severity of the drought event. The recovery time of hydrological drought events is on average twice that of meteorological ones. The variability and high values of recovery rate are especially noticeable in São Francisco (one of the driest regions) and Paraná (a region highly impacted by human activities).

There are several basins for which propagation time are greater than 4 months, which is considerably higher than what has been previously estimated in the literature. It became clear that the propagation time from meteorological drought to hydrological drought can vary considerably depending on the index chosen for the calculation. For example, the difference in timing of onset of meteorological and hydrological droughts is shorter than that using the timing in peak severity or the end of the event. Therefore, while we can have an estimate of the onset of hydrological drought, it is much harder to predict how much longer a hydrological drought will last in comparison to meteorological droughts. These results suggest that only using meteorological droughts is not sufficient to fully characterize droughts. Multi-indicator approaches are necessary to determine the mechanisms of drought development and propagation through the water cycle.

#### CRedit authorship contribution statement

**Alena G. Bevacqua:** Data curation, Conceptualization, Methodology, Software, Visualization, Writing – original draft. **Pedro L.B. Chaffe:** Conceptualization, Methodology, Supervision, Writing – original draft. **Vinicius B.P. Chagas:** Data curation, Visualization, Writing – original draft. **Amir AghaKouchak:** Writing – review & editing.

#### Declaration of Competing Interest

The authors declare that they have no known competing financial interests or personal relationships that could have appeared to influence the work reported in this paper.

#### Acknowledgments

The first author acknowledges the support from the Coordination for the Improvement of Higher Education Personnel (CAPES). The second and third authors acknowledge the support from the Brazilian National Council for Scientific and Technological Development (CNPq).

#### Appendix A. Supplementary data

Supplementary data to this article can be found online at <https://doi.org/10.1016/j.jhydrol.2021.126902>.

#### References

- Apurv, T., Cai, X., 2020. Drought propagation in US watersheds: a process-based understanding of the role of climate and watershed properties. Under Rev. 0–3 <https://doi.org/10.1029/2020WR027755>.
- Bagley, J.E., Desai, A.R., Harding, K.J., Snyder, P.K., Foley, J.A., 2014. Drought and deforestation: Has land cover change influenced recent precipitation extremes in the Amazon? *J. Clim.* 27, 345–361. <https://doi.org/10.1175/JCLI-D-12-00369.1>.
- Barker, L.J., Hannaford, J., Chiveron, A., Svensson, C., 2016. From meteorological to hydrological drought using standardised indicators 20 (6), 2483–2505. <https://doi.org/10.5194/hess-20-2483-2016>.
- Brás, T.A., Jägermeyr, J., Seixas, J., 2019. Exposure of the EU-28 food imports to extreme weather disasters in exporting countries 11 (6), 1373–1393. <https://doi.org/10.1007/s12571-019-00975-2>.
- Brasil Neto, R. M., Santos, C. A. G., Silva, J. F. C. B. da C., da Silva, R. M., dos Santos, C. A. C., Mishra, M., 2021. Evaluation of the TRMM product for monitoring drought over Paraíba State, northeastern Brazil: a trend analysis, 11, 1–18, <https://doi.org/10.1038/s41598-020-80026-5>.
- de Brito, Y.M.A., Rufino, I.A.A., Braga, C.F.C., Mulligan, K., 2021. The Brazilian drought monitoring in a multi-annual perspective 193 (1). <https://doi.org/10.1007/s10661-020-08839-5>.
- Chagas, V. B. P., Chaffe, P. L. B., Addor, N., Fan, F. M., Fleischmann, A. S., Paiva, R. C. D., Siqueira, V. A., 2020. CAMELS-BR: hydrometeorological time series and landscape attributes for 897 catchments in Brazil, 12, 2075–2096, <https://doi.org/10.5194/essd-12-2075-2020>.
- Chatfield, C., 2016. *The Analysis of Time Series*, Chapman and Hall/CRC, 333 pp., <https://doi.org/10.4324/9780203491683>.
- Cunha, A. P. M. A., Zeri, M., Leal, K. D., Costa, L., Cuartas, L. A., Marengo, J. A., Tomasella, J., Vieira, R. M., Barbosa, A. A., Cunningham, C., Cal Garcia, J. V., Broedel, E., Alvalá, R., Ribeiro-Neto, G., 2019. Extreme drought events over Brazil from 2011 to 2019, 10, <https://doi.org/10.3390/atmos10110642>.
- Doughty, C.E., Metcalfe, D.B., Girardin, C.A.J., Amézquita, F.F., Cabrera, D.G., Huasco, W.H., Silva-Espejo, J.E., Araujo-Murakami, A., da Costa, M.C., Rocha, W., Feldpausch, T.R., Mendoza, A.L.M., da Costa, A.C.L., Meir, P., Phillips, O.L., Malhi, Y., 2015. Drought impact on forest carbon dynamics and fluxes in Amazonia 519 (7541), 78–82. <https://doi.org/10.1038/nature14213>.
- Eltahir, E.A.B., Yeh, P.-F., 1999. On the asymmetric response of aquifer water level to floods and droughts in Illinois 35 (4), 1199–1217. <https://doi.org/10.1029/1998WR900071>.
- Getirana, A., 2016. Extreme Water Deficit in Brazil Detected from Space, 17, 591–599, <https://doi.org/10.1175/JHM-D-15-0096.1>.
- Gutiérrez, A.P.A., Engle, N.L., De Nys, E., Molejón, C., Martins, E.S., 2014. Drought preparedness in Brazil 3, 95–106. <https://doi.org/10.1016/j.wace.2013.12.001>.
- Hao, Z., AghaKouchak, A., 2014. A Nonparametric Multivariate Multi-Index Drought Monitoring Framework, 15, 89–101, <https://doi.org/10.1175/JHM-D-12-0160.1>.
- Hayes, M., Svoboda, M., Wall, N., Widhalm, M., 2011. The Lincoln Declaration on Drought Indices: Universal Meteorological Drought Index Recommended, 92, 485–488, <https://doi.org/10.1175/2010BAMS3103.1>.
- Kendall, M.G., 1975. *Rank correlation methods*. Griffin, London, England.
- Mann, H.B., 1945. Nonparametric tests against trend. *Econometrica* 13 (3), 245–259. <https://doi.org/10.2307/1907187>.
- Marengo, J.A., Torres, R.R., Alves, L.M., 2017. Drought in Northeast Brazil—past, present and future 129, 1189–1200. <https://doi.org/10.1007/s00704-016-1840-8>.
- Martens, B., Miralles, D. G., Lievens, H., Van Der Schalie, R., De Jeu, R. A. M., Fernández-Prieto, D., Beck, H. E., Dorigo, W. A., Verhoest, N. E. C., 2017. GLEAM v2: Satellite-based land evaporation and root-zone soil moisture, 10, 1903–1925, <https://doi.org/10.5194/gmd-10-1903-2017>.
- McKee, T. B., Nolan, J., Kleist, J., 1993. The relationship of drought frequency and duration to time scales, 179–184.
- Melo, D. de C. D., Scanlon, B. R., Zhang, Z., Wendland, E., Yin, L., 2016. Reservoir storage and hydrologic responses to droughts in the Paraná River basin, south-eastern Brazil, 20, 4673–4688, <https://doi.org/10.5194/hess-20-4673-2016>.
- Miralles, D.G., Holmes, T.R.H., De Jeu, R.A.M., Gash, J.H., Meesters, A.G.C.A., Dolman, A.J., 2011. Global land-surface evaporation estimated from satellite-based observations 15 (2), 453–469. <https://doi.org/10.5194/hess-15-453-2011>.
- Morales, M. S., Cook, E. R., Barichivich, J., Christie, D. A., Villalba, R., LeQuesne, C., Srur, A. M., Ferrero, M. E., González-Reyes, A., Couvreur, F., Matkovsky, V., Aravena, J. C., Lara, A., Mundo, I. A., Rojas, F., Prieto, M. R., Smerdon, J. E., Bianchi, L. O., Masiokas, M. H., Urrutia-Jalabert, R., Rodríguez-Catón, M., Muñoz, A. A., Rojas-Badilla, M., Alvarez, C., Lopez, L., Luckman, B. H., Lister, D., Harris, I., Jones, P. D., Williams, A. P., Velazquez, G., Aliste, D., Aguilera-Betti, I., Marcotti, E., Flores, F., Muñoz, T., Cui, E., Boninsegna, J. A., 2020. Six hundred years of South American tree rings reveal an increase in severe hydroclimatic events since mid-20th century, 117, 16816–16823, <https://doi.org/10.1073/pnas.2002411117>.
- Paredes-Trejo, F., Barbosa, H.A., Giovannetone, J., Lakshmi Kumar, T.V., Thakur, M.K., de Oliveira Burity, C., 2021. Long-Term Spatiotemporal Variation of Droughts in the Amazon River Basin 13 (3), 351. <https://doi.org/10.3390/w13030351>.
- Rodrigues, J.A.M., Viola, M.R., Alvarenga, L.A., Mello, C.R., Chou, S.C., Oliveira, V.A., Uddameri, V., Morais, M.A.V., 2020. Climate change impacts under representative concentration pathway scenarios on streamflow and droughts of basins in the Brazilian Cerrado biome 40 (5), 2511–2526. <https://doi.org/10.1002/joc.v40.510.1002/joc.6347>.
- Sen, P.K., 1968. Estimates of the Regression Coefficient Based on Kendall's Tau 63 (324), 1379–1389. <https://doi.org/10.1080/01621459.1968.10480934>.
- Shukla, S., Wood, A.W., 2008. Use of a standardized runoff index for characterizing hydrologic drought 35, 1–7. <https://doi.org/10.1029/2007GL032487>.

- Stagge, J.H., Tallaksen, L.M., Gudmundsson, L., Van Loon, A.F., Stahl, K., 2015. Candidate Distributions for Climatological Drought Indices (SPI and SPEI) 36, 2132–2138. <https://doi.org/10.1002/joc.4564>.
- Taufik, M., Torfs, P.J.J.F., Uijlenhoet, R., Jones, P.D., Murdiyarso, D., Van Lanen, H.A.J., 2017. Amplification of wildfire area burnt by hydrological drought in the humid tropics 7 (6), 428–431. <https://doi.org/10.1038/nclimate3280>.
- Theil, H., 1950. A rank-invariant method of linear and polynomial 392, 387–.
- USGS - U.S. GEOLOGICAL SURVEY. Shuttle Radar Topography Mission 1 Arc Second scene. Maryland, USA: 2006. Available in: <<http://earthexplorer.usgs.gov/>>. Accessed in: 10 jun. 2017.
- Van Lanen, H.A.J., Wanders, N., Tallaksen, L.M., Van Loon, A.F., 2013. Hydrological drought across the world: impact of climate and physical catchment structure. *Hydrol. Earth Syst. Sci.* 17, 1715–1732. <https://doi.org/10.5194/hess-17-1715-2013>.
- Van Loon, A.F., Laaha, G., 2014. Hydrological drought severity explained by climate and catchment characteristics. *J. Hydrol.* 526, 3–14. <https://doi.org/10.1016/j.jhydrol.2014.10.059>.
- Van Loon, A.F., 2015. Hydrological drought explained 2 (4), 359–392. <https://doi.org/10.1002/wat2.2015.2.issue-410.1002/wat2.1085>.
- Van Loon, A.F., Gleeson, T., Clark, J., Van Dijk, A.I.J.M., Stahl, K., Hannaford, J., Di Baldassarre, G., Teuling, A.J., Tallaksen, L.M., Uijlenhoet, R., Hannah, D.M., Sheffield, J., Svoboda, M., Verbeiren, B., Wagener, T., Rangelcroft, S., Wanders, N., Van Lanen, H.A.J., 2016. Drought in the Anthropocene 9 (2), 89–91. <https://doi.org/10.1038/ngeo2646>.
- Vicente-Serrano, S. M., Beguería, S., and López-Moreno, J. I., 2010. A Multiscalar Drought Index Sensitive to Global Warming: The Standardized Precipitation Evapotranspiration Index, 23, 1696–1718, <https://doi.org/10.1175/2009JCLI2909.1>.
- Vicente-Serrano, S.M., López-Moreno, J.I., Beguería, S., Lorenzo-Lacruz, J., Azorin-Molina, C., Morán-Tejeda, E., 2012. Accurate Computation of a Streamflow Drought Index 17 (2), 318–332. [https://doi.org/10.1061/\(ASCE\)HE.1943-5584.0000433](https://doi.org/10.1061/(ASCE)HE.1943-5584.0000433).
- Wilhite, D.A., 2000. Drought as a Natural Hazard 1, 3–18.
- Wilhite, D.A., Glantz, M.H., 1985. Understanding the Drought Phenomenon: The Role of Definitions 10 (3), 111–120. <https://doi.org/10.1080/02508068508686328>.
- Wilhite, D. A. and Pulwarty, R. S.: Drought and Water Crises, edited by: Wilhite, D. and Pulwarty, R. S., CRC Press, Second edition. | Boca Raton : CRC Press, 2018. 1st ed. published in 2005. <https://doi.org/10.1201/b22009>, 2018.
- WMO, 2014. Atlas of Mortality and Economic Losses from Weather, Climate and Water Extremes, 48 pp., [https://doi.org/ISBN 978-92-63-11123-4](https://doi.org/ISBN%20978-92-63-11123-4).
- Wu, J., Miao, C., Zheng, H., Duan, Q., Lei, X., Li, H.u., 2018. Meteorological and Hydrological Drought on the Loess Plateau, China: Evolutionary Characteristics, Impact, and Propagation 123 (20), 11,569–11,584. <https://doi.org/10.1029/2018JD029145>.
- Wu, J., Chen, X., Love, C.A., Yao, H., Chen, X., AghaKouchak, A., 2020. Determination of water required to recover from hydrological drought: Perspective from drought propagation and non-standardized indices 590, 125227. <https://doi.org/10.1016/j.jhydrol.2020.125227>.
- Wu, J., Chen, X., Yuan, X., Yao, H., Zhao, Y., AghaKouchak, A., 2021. The interactions between hydrological drought evolution and precipitation-streamflow relationship 597, 126210. <https://doi.org/10.1016/j.jhydrol.2021.126210>.
- Xavier, A.C., King, C.W., Scanlon, B.R., 2016. Daily gridded meteorological variables in Brazil 36 (6), 2644–2659. <https://doi.org/10.1002/joc.2016.36.issue-610.1002/joc.4518>.
- Xu, Y., Zhang, X., Wang, X., Hao, Z., Singh, V.P., Hao, F., 2019. Propagation from meteorological drought to hydrological drought under the impact of human activities: A case study in northern China 579, 124147. <https://doi.org/10.1016/j.jhydrol.2019.124147>.
- Zeng, X., Zhao, N.a., Sun, H., Ye, L., Zhai, J., Dias, J.M., 2015. Changes and relationships of climatic and hydrological droughts in the Jialing River basin, China 10 (11), e0141648. <https://doi.org/10.1371/journal.pone.0141648>. <https://doi.org/10.1371/journal.pone.0141648.s00110.1371/journal.pone.0141648.s00210.1371/journal.pone.0141648.s00310.1371/journal.pone.0141648.s00410.1371/journal.pone.0141648.s00510.1371/journal.pone.0141648.s00610.1371/journal.pone.0141648.s00710.1371/journal.pone.0141648.s00810.1371/journal.pone.0141648.s00910.1371/journal.pone.0141648.s01010.1371/journal.pone.0141648.s01110.1371/journal.pone.0141648.s01210.1371/journal.pone.0141648.s01310.1371/journal.pone.0141648.s01410.1371/journal.pone.0141648.s01510.1371/journal.pone.0141648.s016>.
- Zhou, J., Li, Q., Wang, L., Lei, L.i., Huang, M., Xiang, J., Feng, W., Zhao, Y., Xue, D., Liu, C., Wei, W., Zhu, G., 2019. Impact of climate change and land-use on the propagation from meteorological drought to hydrological drought in the eastern Qilian Mountains 11 (8), 1602. <https://doi.org/10.3390/w11081602>.